

Plasma Focusing of the Final Focus Test Beam*

S. Rajagopalan*

Stanford Linear Accelerator Center, Stanford University, Stanford, CA 94309

Abstract

The focusing of the Final Focus Test Beam by means of a plasma is studied by means of models, based on theory and simulation. A set of parameters for a test of various aspects of plasma focusing is presented with attention to the limitations of diagnostic schemes available presently at the FFTB.

I. INTRODUCTION

Plasma focusing devices are compact, simple, and very strong focusing elements. The focusing strengths for typical parameters are equivalent to $\sim 10^9$ Gauss/cm focusing magnets. In principle, such strong fields are capable of focusing beams to very small spot sizes. Several proof-of-principle experiments using low density particle beams have demonstrated plasma focusing. The goal in this paper is to define a set of parameters for a plasma lens test using the FFTB. The results will be of interest for SLC and the next generation high energy linear colliders.

For our purposes, the focusing nature of the interaction can be understood using the following arguments without detailed mathematical analysis: The beam particles carry charge and current. For a relativistic beam in vacuum the electric repulsion is almost neutralized by the magnetic attraction among the particles. The introduction of the beam into the plasma results in a response that neutralizes the intrusion as much as possible. The charge neutralization takes place primarily by the fast motion of the plasma electrons and the current neutralization occurs due to the development of the "return current" in the plasma. The resulting large electric and magnetic fields both accelerate and focus trailing particles. For a single bunch the head can excite the plasma and focus the main body of the bunch.

II. Model of Focusing

The focusing strength of a plasma lens depends on whether it is underdense or overdense. When ignoring the effects due to the return current, the focusing strength for underdense lenses is governed by the plasma density n_p ,

$$K = \frac{2\pi r_e}{\gamma} n_p,$$

* Work supported by the U.S. Department of Energy under contract DE-AC03-76SF00515 and grant DE-AS03-88ER40381.

* Visitor from Department of Physics, UCLA, Los Angeles, CA 90024.

whereas for overdense lenses the strength is determined by the beam density n_b ,

$$K = \frac{2\pi r_e}{\gamma} n_b.$$

However the formula for an overdense plasma is true only in the extreme where the period of plasma oscillations is much smaller than the time of passage of the beam and the amplitude is much smaller than the beam radius. The change in beam density is taken into account as the beam propagates in the plasma. The equation used for the beta function is

$$\beta''' + 4K\beta' + 2K'\beta = 0$$

The boundary conditions are that β and β' are continuous and at the boundary of the lens the quantity $\beta'' + 4K\beta$ jumps by $2\Delta K\beta$, where ΔK is the discontinuity in K . The beta function can be found by numerically integrating with the proper boundary conditions and plasma regimes.

The longitudinal variation of beam density is taken into account by calculating the beta functions of different slices of the beam. In the regime where the focusing dynamics changes from underdense to overdense there is a transition where the oscillation of the plasma gives rise to focusing beyond the limit imposed by the beam density. This is seen to be true upto a density ratio of plasma to beam of 2. Therefore a conservative model limits the focusing strength to twice that from a plasma of density twice the beam. This is true for the range of beam densities under study.

The transverse variation in focusing strength due to incomplete expulsion of plasma electrons is not included in this model. Like the longitudinal effects this affects only the tails of the distribution. One transverse effect, that of return currents in the extreme overdense case is included and the effect for Case C is in Table 1. This flows outside the beam in all other cases and can be ignored except in case C where the plasma oscillations are much faster than the time of passage of the beam and the current penetrates the beam volume.

The evolution of the integrated beam sizes in Case A thru E are calculated with the effects of the longitudinal variation included, as shown in Figures 1 thru 5 respectively.

III. Round Beam Focusing

The plasma is created by an intense laser beam before the arrival of the particle beam bunch. The gas target density will be varied to cover all regimes of the plasma lens from underdense to overdense and to the

regime where the effect of current neutralization can be observed in the focusing. The optimized lens conditions will be capable of demonstrating the focusing of a $5 \mu\text{m}$ round beam to a final spot size of about $2 \mu\text{m}$. A fully coupled "round beam" in the FFTB line is assumed to have the normal FFTB population of 1×10^{10} per bunch at 10 Hz. The results are summarised in Table 1 below.

Table 1

Beam	A	B	C
$\mathcal{E}[\text{GeV}]$	50	50	50
$N[10^{10}]$	1.0	1.0	1.0
$\epsilon_n[10^{-5}\text{m} - \text{rad}]$	3.0	3.0	3.0
$\beta_0^*[\text{cm}]$	7.5	7.5	7.5
$\sigma_{r0}^*[\mu\text{m}]$	4.74	4.74	4.74
$\beta_0[\text{cm}]$	8.03	8.03	8.03
$\sigma_0[\mu\text{m}]$	4.91	4.91	4.91
$\sigma_z[\text{mm}]$	0.47	0.47	0.47
$n_{b0}[10^{16}\text{cm}^{-3}]$	5.3	5.3	5.3
Lens			
$n_p[10^{17}\text{cm}^{-3}]$	0.2	1.0	10
$k_p\sigma_z$	12.5	28.0	88.5
$s_0[\text{cm}]$	-2.0	-2.0	-2.0
$l[\text{cm}]$	0.3	0.3	0.3
$f[\text{cm}]$	3.80	2.92	3.60
Focused Beam			
$\beta_r^*[\text{mm}]$	3.7	2.1	3.4
$\sigma_r^*[\mu\text{m}]$	3.35	2.55	3.23
$s^*[\text{cm}]$	1.95	1.07	1.75

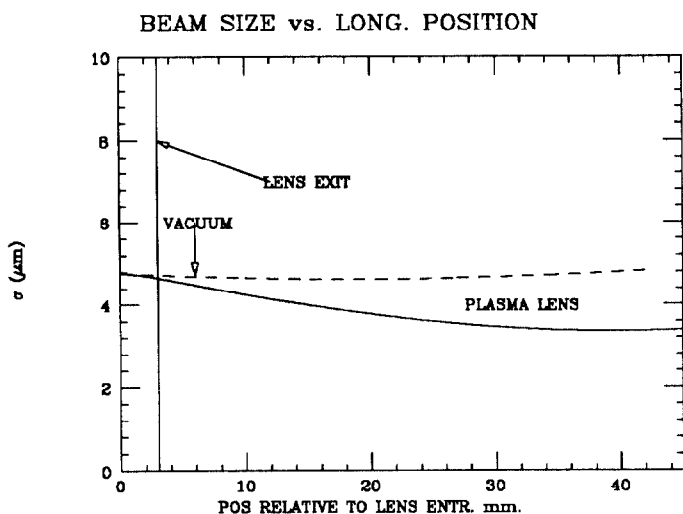


Figure 1. Underdense lens. Solid line includes long. effects. Dashed line is vacuum and dotdash is plasma lens without aberrations.

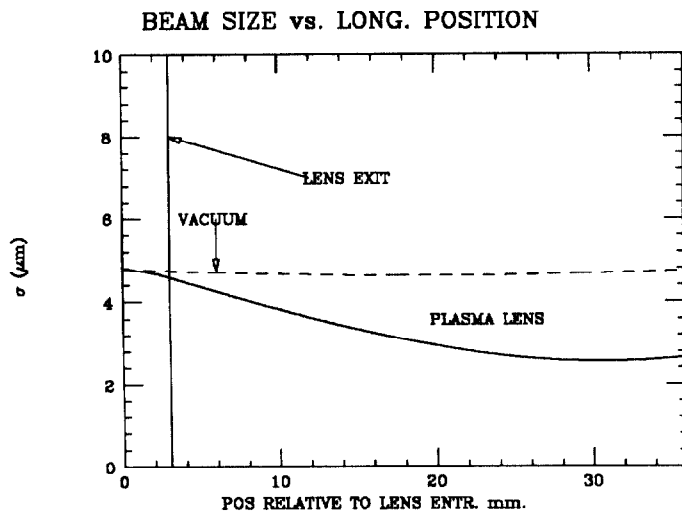


Figure 2. Mostly undersense lens. Solid line includes long. effects. Dashed line is vacuum and dotdash is plasma lens without aberrations.

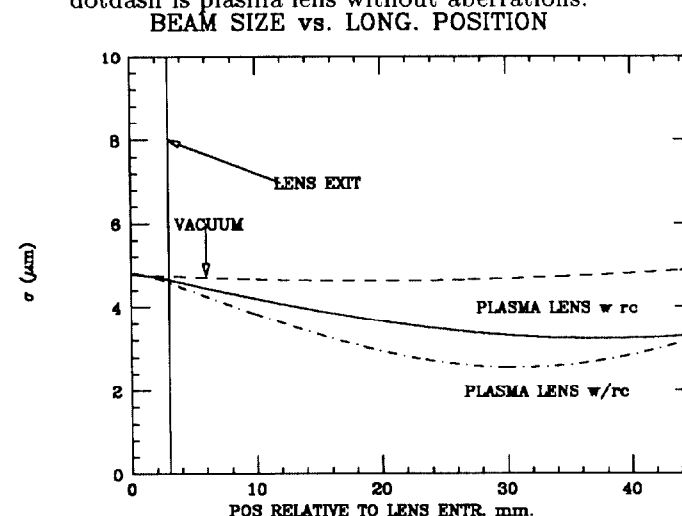


Figure 3. Overdense lens. Solid line includes long. effects. Dashed line is vacuum and dotdash is plasma lens without aberrations. The spot size is degraded due to return currents from $2.55 \mu\text{m}$ to $3.23 \mu\text{m}$.

IV. Flat Beam Focusing

This is to study the focusing of the beam with a laser-ionized plasma and also a beam-ionized plasma. The bunch population is increased to 2.5×10^{10} per bunch while maintaining the aspect ratio of the FFTB i.e., $\epsilon_{nx}/\epsilon_{ny} = 3 \times 10^{-5}\text{m} - \text{rad}/3 \times 10^{-6}\text{m} - \text{rad}$. This will help to improve the impact ionization probability and to reach the tunneling ionization threshold. Two cases are presented for testing focusing by tunnelling ionization and to focus better than the FFTB. The former case has a relaxed beta function for the y direction to prevent a rapid blowup of the beam. The results are summarised in Table

Table 2

Beam	D	E
$N[10^{10}]$	2.5	2.5
$\epsilon_{nx}/\epsilon_{ny}[10^{-5}\text{mrad}]$	3.0 / 0.3	3.0 / 0.3
$\beta_{x0}^*/\beta_{y0}^*[\text{mm}]$	3.0 / 3.0	3.0 / 0.12
$\sigma_{x0}^*/\sigma_{y0}^*[\text{nm}]$	1000 / 333	1000 / 60
$\beta_{x0}/\beta_{y0}[\text{mm}]$	4.33 / 4.33	4.33 / 33.5
$\sigma_{x0}/\sigma_{y0}[\text{nm}]$	1200 / 400	1200 / 1000
$n_{b0}[10^{18}\text{cm}^{-3}]$	7.7	2.8
Lens		
$n_p[10^{18}\text{cm}^{-3}]$	2.0	2.5
$s_0[\text{mm}]$	-2	-2
$l[\text{mm}]$	1	1
Focused Beam		
$\beta_x^*/\beta_y^*[\text{mm}]$	0.90 / 0.90	0.75 / 0.047
$\sigma_x^*/\sigma_y^*[\text{nm}]$	520 / 165	480 / 38
$s_x^*/s_y^*[\text{mm}]$	0.10 / 0.10	-0.12 / -0.63

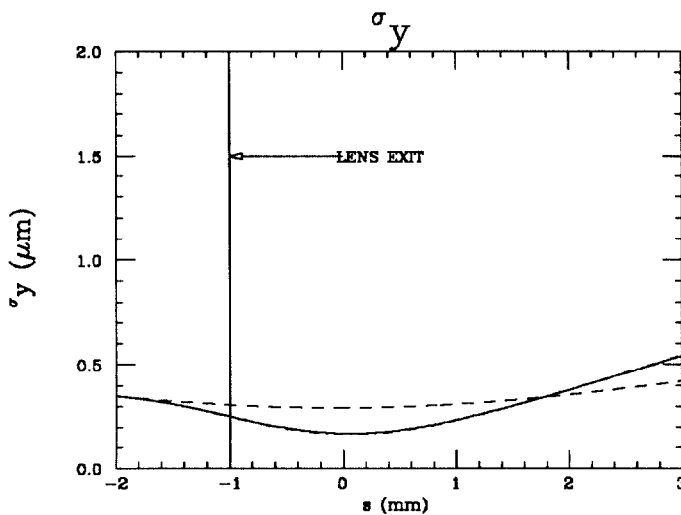


Figure 4. Focusing with a beam-ionized plasma produced with a relaxed β_y .

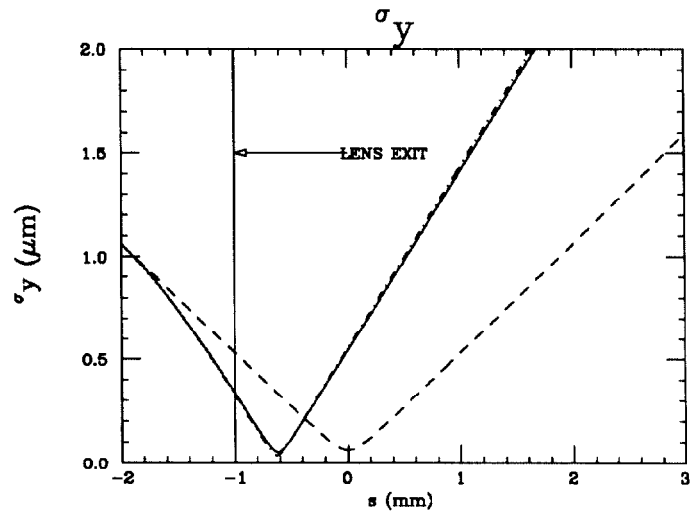
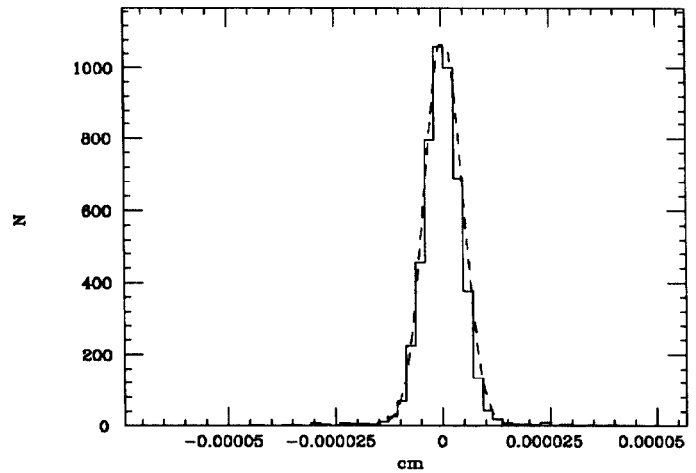


Figure 5. Focusing to improve on the FFTB. Longitudinal effects degrade σ_y^* to 55 nm. But a plot of the particles shows the core is best fitted by a Gaussian with σ between 40 and 45 nm. This can be distinguished from 60 nm by the Compton backscattering monitor.
Histogram of particles at Focal Point



V. Comments

The plasma lenses in our experiments produce beam sizes in the range of $\sim 40 \text{ nm} - 4 \mu\text{m}$, thus beam size and profile measurements over this range will be required. For Case A thru C the focused beam sizes are in the $\sim 2 - 4 \mu\text{m}$ range and can be conveniently measured with a wire scanner. The beam sizes are determined from the bremsstrahlung yields as the electron beam is scanned across micron sized fibers. The sub-micron focused beam sizes for Case D and E can be measured with a Compton Backscattering monitor. I would like to acknowledge help and comments from P. Chen, R. Ruth, P. Kwok, D. Cline and others whom space precludes mention.

VI. REFERENCES

All the references contained in "Plasma lens Experiments at the Final Focus Test Beam" in these same proceedings.